Journal of Constructional Steel Research 115 (2015) 407–416

Contents lists available at ScienceDirect

Journal of Constructional Steel Research

Welding of girders with thick plates — Fabrication, measurement and simulation

H. Pasternak, B. Launert *, T. Krausche

Brandenburg University of Technology, Cottbus, Germany

ARTICLE INFO

Article history:
Received 7 April 2015
Received in revised form 24 July 2015
Accepted 27 August 2015
Available online 14 September 2015

Keywords:
Welded plate girders
Welding simulation
Residual welding stress
Load capacity

ABSTRACT

This article presents experimental and numerical results of the fabrication of welded plate girders under workshop conditions. Main concerns are the prediction of imperfections with the aid of simulation tools and/or simplified engineering models. Their impact on the component design is evaluated in a case study. Special focus is put on the effect of residual welding stress. For this, different simplified distributions are compared with results from welding simulation. The findings confirm the thesis that present recommendations on the implementation of weld-induced imperfections must be rated conservative. This suggests that it is necessary to establish new models. Guidance on future problems in this context will be given.

1. Indroduction

In steel construction, usually the production contains two stages: the manufacture of parts under workshop conditions and the assembly on site. The former can be partially automated and has a much higher level of reliability compared to site welds. This article addresses the manufacture of such girders and proceeds to the production in the factory and the simulation of the welding process. Results in terms of residual stress and distortion are given and compared with typical engineering models. The validation of models is based on experimental data obtained during and after the manufacture. For a subsequent capacity analysis results are idealized and then implemented as initial conditions. The comparison of different models allows a review of recent standards. All results were obtained in the scope of a common research project of Brandenburg University of Technology and the University of Braunschweig (ifs).

2. Manufacture and measurements

The manufacture of the girders was performed under workshop conditions. Fig. 1 documents the geometry of the test specimens. Since the project consists of two parts, all examined girders received additional preparation for the assembly of two components in a Z-joint. Below, only the girder fabrication is discussed. The length of specimens was chosen with respect to the formation of a stationary stress state representative for girders with long longitudinal welds. The source materials are sheets of P355NL2. The sheets were delivered cut to size and with weld preparation (EN ISO 9692). To account for the assumption of an approximately stress-free state, all sheets were saw cut. This was confirmed by measurements prior to welding [1]. For further information on the influence of the cutting procedure, particularly if the use of concentrated amounts of heat is involved (e.g. flame or plasma cutting) see [2]. Thickness is 30 mm for the upper and lower flange and 15 mm for the web. Flange width is 500 mm and web height 800 mm. Due to the assembly of girders, which was realized as a second part of the project, all dimensions are in accordance with the restrictions given by the testing facility. The results for the assembly of girders can be found in [1].

Welding of fillet welds is performed in one layer with a throat thickness a = 5 mm. The process 135 (EN ISO 4063), metal active gas welding (MAG) with solid wire electrode, was used, because this is the most widely used process for factory fabrication work. An overview of the parameters is shown in Table 1. A total of 6 girders were manufactured. The fabrication took place in a manufacturing company in Dessau, Germany. Fig. 2 presents an example for the girder manufacture. No preheating was performed.

Fig. 3 shows the macrosection of a T-joint, which was welded with the same parameters as recorded during manufacture. According to the classification in EN ISO 5817, welds correspond to quality level B. The quality level, indicated by letters B (highest requirement), C or D (lowest requirement), specifies the quality of a weld based on type, size and number of irregularities. For steel constructions, EN 1090-2 contains additional specifications, indicated by the execution class (EXC) 1 to 4. The execution class can be defined for the whole structure or parts of the structure.

The welds were deposited manually one at a time. In practical applications with long continuous welds this is realized fully mechanized. The manufacture was monitored. The temperature was measured

* Corresponding author.
E-mail address: benjamin.launert@b-tu.de (B. Launert).

http://dx.doi.org/10.1016/j.jcsr.2015.08.037
0143-974X/

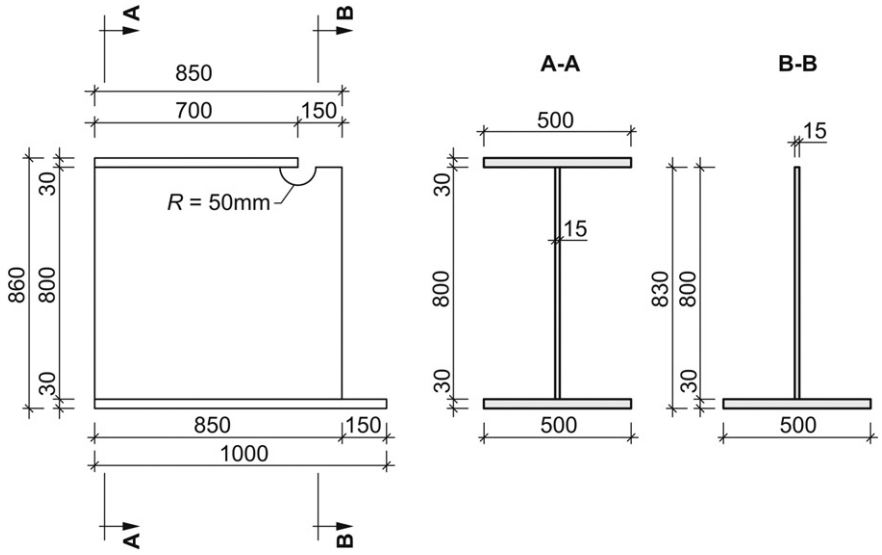

Fig. 1. Geometry of the specimens (note: the assembly of girders in a Z-joint is presented in [1]).

using type K thermocouples (range of temperature up to +1100 °C, for a short time up to +1300 °C). The temperature cycles are important to calibrate the heat input to the numerical model in Section 3 (e.g. efficiency). During the whole process distortions were also measured using inductive displacement sensors. Figs. 4 and 5 present temperature and distortion measurements representative for the testing of girders P355NL2. After welding residual stress was measured using X-ray diffraction (XRD). This method is based on measuring the diffraction angle, which is used to determine the interplanar spacing. Mechanical stress leads to very small changes in the lattice spacings only (<0.1%); therefore the diffraction angle must be determined with an accuracy of about 0.01 to 0.5°. The penetration depth is strictly limited (up to 5 μm), which is why results are restricted to the surface. Because of the dimensions a mobile diffractometer from ifs was used. Stress distributions longitudinal and transverse to the weld seam direction were determined. The data are important input quantities for the validation of numerical welding simulation models. The evaluation of experimental data has shown that results are comparable for all girders manufactured [1].

3. Welding simulation

3.1. Theoretical principles

The welding simulation has made a large progress in recent years. It allows the understanding of complex interactions during welding and cooling and thereby a more targeted optimization of the design. In the following, aspects of structural welding simulation are discussed. The macro behaviour under local heat input is simulated. The simulation can be performed using different multi-purpose or specialized software tools. Fig. 6 illustrates the typical calculation flow.

One of the basic assumptions is the weak coupling between thermo-physical and thermo-mechanical sub-models, i.e. temperature field, composition of microstructure and mechanics are determined in separate runs. The thermal analysis is based on the solution of the heat transfer equation. The heat source is idealized using mathematical models describing the distribution of heat. The most typical approach is presented by Goldak [3]. The geometric parameters of the source distribution are calibrated based on experimental data (melt zone and thermal cycles). The heat is dissipated by thermal conduction within the component as well as radiation and convection on the surface. Thermo-physical data such as thermal conductivity, specific heat and density are temperature dependent and therefore needed as a function of temperature. During phase change, a considerable amount of heat is released or absorbed (latent heat), causing a strong non-linearity in the specific heat function. Instead usually the specific or volume specific enthalpy function is used.

In a fully transient analysis the temperature field is transferred to an adequate mechanical model (the same mesh, but different element types, material properties and boundary conditions) for each time step. The mechanical solution is particularly time consuming. Input quantities are the calculated temperatures (or thermal strains respectively) and, for models taking into account the transformation of the microstructure, also transformations strains (resulting from the volume change during austenite transformation) and plastic strains due to the effect of transformation plasticity. To account for phase transformation effects different semi-empirical and empirical models can be used. The

Table 1
Overview of manufacturing parameters (P355NL2).

I [A]	U [V]	v_{Weld} [cm/min]	v_{Wire} [m/min]	Welding process	Welding position	Filler material
280–290	33	28.57	10	135	PB	G4Si1

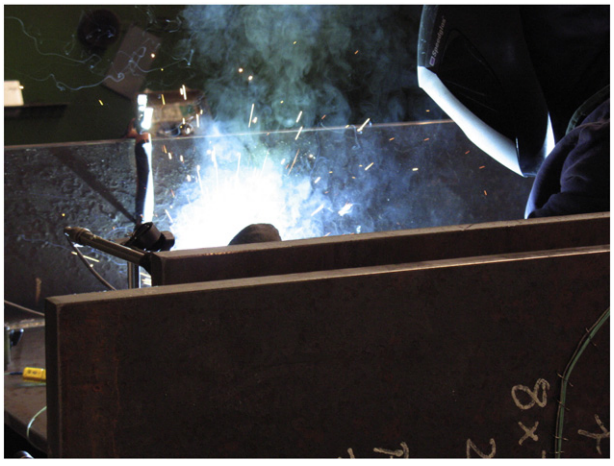

Fig. 2. Manufacturing under workshop conditions (Stahlbau Dessau GmbH & Co. KG, Germany).

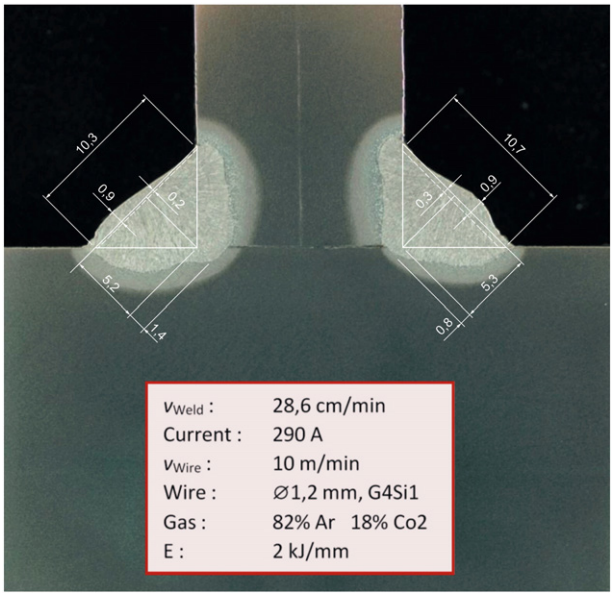

Fig. 3. Transverse macrosection for laboratory sample and dimensions of fillet welds (quality level B, EN ISO 5817).

semi-empirical model of Leblond and Devaux [4] is a commonly used approach. This model is based on the equations by Johnson–Mehl–Avrami [5] for diffusion-oriented transformations and Koistinen and Marburger [6] for martensitic transformation. The parameters required for this model are determined from continuous cooling transformation (CCT) diagrams. Based on a mixing rule and the calculated phase composition the set of material data is modified for each element. Hence, for the calculation of structure mechanics the material data are a function of temperature and in addition a function of the material composition. Data are provided for ferrite–perlite, bainite, martensite and austenite.

Thermo-mechanical material data are the yield strength, the coefficient of thermal expansion (both as a function of temperature and microstructure), the Young's modulus (usually introduced without dependency on the microstructure) and the Poisson's ratio (assumed constant, for steel 0.3). The plasticity law may consider either isotropic or kinematic hardening; the calculation of yield stress is based on v. Mises. The corresponding stress–strain curves are defined as multilinear curves (or bilinear curves if simplified). Data for S355 can be found in literature, e.g. hot tensile tests from Peil and Wichers [7]. For martensite and bainite the functions are scaled according to the ratio of yield stress at room temperature (related to the base material). For austenite the stress–strain curve can be taken from X5CrNi 18 10 [8].

The elements used for the thermal and mechanical sub-models are three-dimensional isoparametric elements with linear shape functions. The spatial and time discretizations of the model are adapted with regard to the particular task. A welding oriented mesh involves the consideration of high gradients, which can occur for the temperature, the stress (or likewise strain) distribution as well as the composition of the microstructure. This is realized applying a fine mesh in the weld area and the heat affected zone (HAZ). Remaining parts can be mapped by larger elements. Generally about 70% of the elements should be located in the area where plastic deformation occurs. Besides the spatial discretization computation time strongly depends on the analysis period (welding and cooling) as well as the size of time steps. The latter is limited due to length of the weld pool which mainly depends on the process. With an increase in model size and the length of welds, the computation time increases considerably.

The described correlations are presented in detail in [9]. Due to the simplifications for the simulation of the welding process, calibration with experiments is necessary.

3.2. Welding simulation model

The numerical welding simulation model of the specimen in SYSWELD is shown in Fig. 7. The model was created by ifs. Calculation was realized using symmetry condition. Introducing symmetry to the model would require that the system and the loads (loads may be illustrated better by an imaginary shrinkage force in this context) are symmetric. Assuming that all welds were deposited simultaneously it is enough to model a quarter of the system. If two adjacent welds were deposited at the same time, a vertical symmetry plane about the web axis may be introduced. On the other hand, a horizontal symmetry plane at half web height may be introduced, if welds on one site of the girder are deposited simultaneously. The latter is used in this model. It should be noticed that this assumption is not appropriate in a strict sense (as welds are deposited one at a time). However, due to the web height in this example (800 mm) fillet welds do not affect one another. It should be highlighted here that the focus of the model was a study on the residual stress state.

The length of the weld path has been set differently from that shown in Fig. 1. A length of 525 mm was chosen. This was the minimum length to achieve a stationary stress state in the middle of the specimen, where the residual stress distribution is evaluated later. For meshing hexahedral elements with linear shape functions were used. In total, the model consists of 135,896 elements. The welding parameters are the same as presented in Table 1. The efficiency is a calibration factor in the numerical simulation (affecting mainly the global distribution of temperature). If no experimental data is available, one would assume 0.8 for MAG process. The temperature field in the weld region is affected by the distribution of heat. The heat source is described using 2 quarter ellipsoids with normally distributed heat generation rate (Goldak). Details are included in [1]. The material data base covers a wide range of materials. For the simulation the material data set S355_Tempering

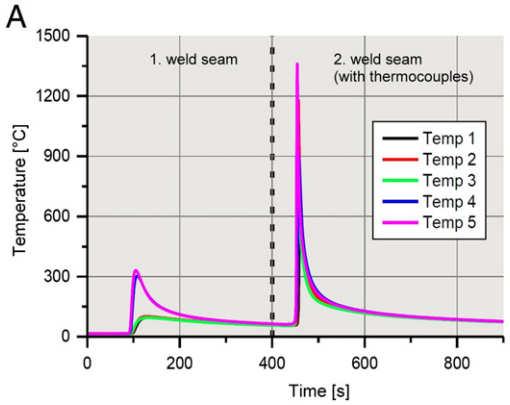

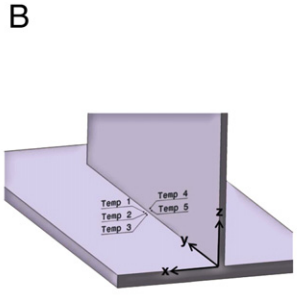

	x [mm]	y [mm]	z [mm]
Temp 1	10	456	0
Temp 2	9	445	0
Temp 3	10,5	433	0
Temp 4	0	442	11,5
Temp 5	0	433	9

Fig. 4. Measured temperature cycles (Temp 1–Temp 5) during welding and cooling, exemplary for P355NL [1].

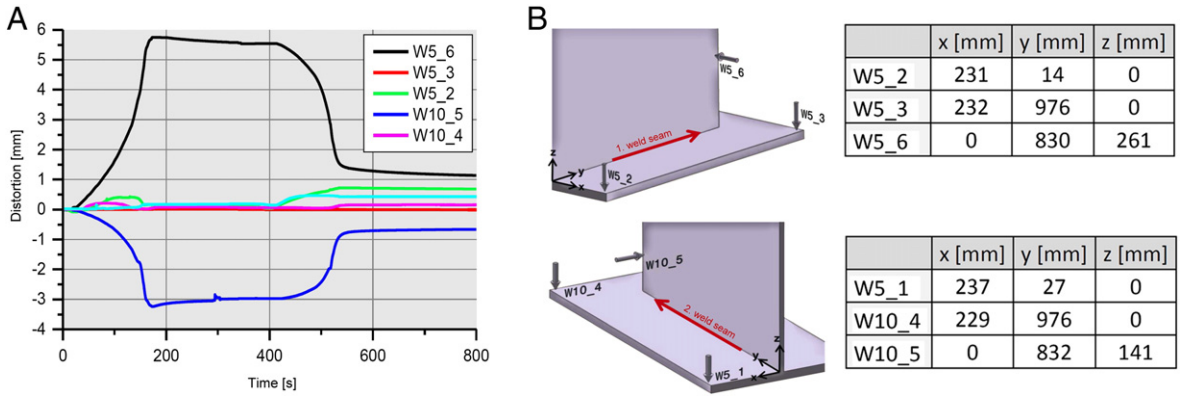

	x [mm]	y [mm]	z [mm]
W5_2	231	14	0
W5_3	232	976	0
W5_6	0	830	261

	x [mm]	y [mm]	z [mm]
W5_1	237	27	0
W10_4	229	976	0
W10_5	0	832	141

Fig. 5. Measured deformations at selected points, exemplary for P355NL2 [1].

in SYSWELD was used. Material quantities are equal to those of the examined steel grade P355NL2. For the weld joint an initial gap of 0.5 mm is assumed.

Fig. 8 shows the results of the thermal solution in comparison to the melt pool dimensions obtained from the macrosection. A good correlation between simulation and experimental results can be seen. The mechanical response in terms of residual stress is plotted for the upper flange in Fig. 9. The blue graph corresponds to the measured distribution. As a result of the restriction in the accessibility of the diffractometer, experimental values are only given for the outer surface, respectively for the lower and upper flange. The partial variation of measured stress is caused by the rolling skin and the corrosion on the surface of the specimens (and therefore must be interpreted as measuring error). On average, a good correlation is achieved. To study the influence of a variation in thickness, Fig. 10 shows the course of simulated longitudinal residual stress at 4 sections.

The maximum stress level close to the weld is about 400 to 600 MPa, base material is S355. This is caused due to phase transformation effects in the heat affected zone (i.e. bainitic and martensitic transformation) and due to the plasticity model used (model with isotropic hardening). The influence of transformation-induced stress components on the overall result is negligible in this example due to the relatively small value of the hot yield strength for mild steel and the high transformation temperature in comparison to high-strength steels, which is confirmed by the results. An experimental validation for the stresses close to the weld was not possible as the interior surface of the flange could not be accessed by the diffractometer without sectioning the specimen.

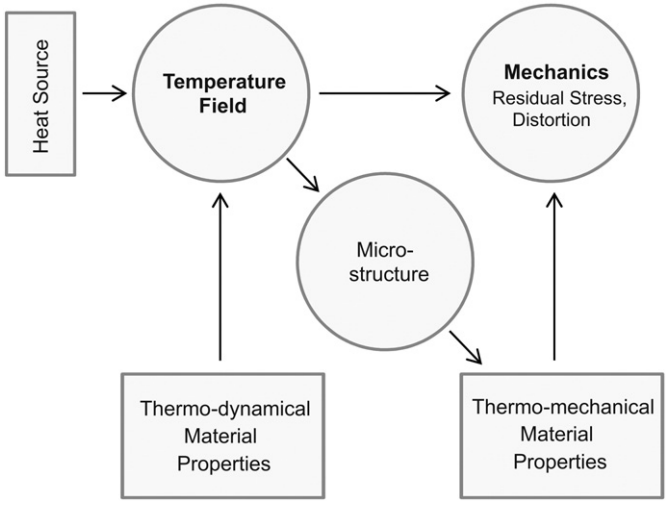

Fig. 6. Calculation chart for structural welding simulation (thermo-mechanical analysis with weak coupling) [9].

With regard to the welding of thick metal sheets, here $t_f = 30$ mm, usually a strong gradient across the thickness can be noticed. Its occurrence mainly depends on the ratio of heat input and thickness. Especially close to the weld a significant variation in stress can be seen. In contrast, a relatively homogeneous stress distribution is noticed for the web ($t_w = 15$ mm). The component behaviour (see Section 5) is primarily influenced by the compressive residual stress field. The evaluation shows only a slight variation in stress. Therefore the course of stress is approximated in Fig. 11 assuming a constant stress level over the thickness. It should be noted carefully, that a single section may be in a non-equilibrium state as the equilibrium is generally fulfilled in volume. The given distribution reflects only an average stress state for the tensile and compressive stress field. The comparison with simplified models used for the capacity analysis is presented in Section 4.

Another major aspect in terms of the component behaviour is the resulting distortion indicated as initial geometrical imperfections. In Fig. 12 the total distortion is illustrated with 50× magnification. A comparison with values proposed by the standard is presented in Section 4. As the length of the girder is comparatively small, conclusions are limited to local distortions.

As a complement several simplified models have been developed in Simufact (version 3.1.1). To study the influence of the mesh density the element edge length in the weld area and the HAZ was varied between 1 to 5 mm. For seam distant areas the element edge length was chosen as 10 mm. As an example the mesh 2.5–10 mm is documented in Fig. 13. For this purpose, a good approximation to the experimental curve was obtained. Lower mesh density led to deviations of the stress state close to the weld and is therefore not recommended. The consideration of transformation effects resulted in no significant change. Dependent on the transformation behaviour of the steel and the cooling rate, the influence for other cases can be larger and may need consideration.

3.3. Conclusions — welding simulation

As a result of the constant progress made in this field, a realistic prediction of welding distortion and residual stress is possible. Of course partially variation is random, since particular conditions may vary for practical cases. However, for the manufacture of girders, which is preferably carried out mechanized and therefore has only little statistical scatter, it seems logical to use the potential given by available simulation tools. Nevertheless, a larger application in steel construction still remains uncertain as the calculation effort and consequently the costs usually do not balance the benefits gained by such analysis. At the same time the size of models is restricted to small components. The application to large structures with several meters of weld length is hardly possible today. Therefore the use of adequate engineering models is of particular importance. A selection of models is given in the next section.

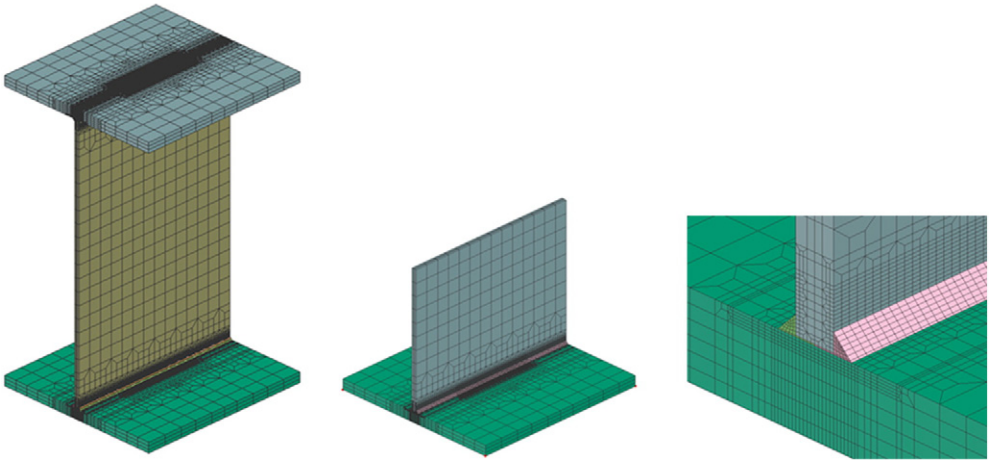

Fig. 7. Numerical model of the complete and half part demonstrator (S355_Tempering) [1], Sysweld.

4. Engineering Models

The result of the capacity calculation is significantly influenced by the imperfection approach. This term includes any production-related deviation from the ideal state. In terms of welding those are distortions and residual stress as well as changes of the microstructure within the HAZ. In the context of the Eurocode 3 (EC3) these phenomena are regarded as geometrical and structural imperfections. According to EC3, Part 1–5, Annex C, the former may be introduced as eigenmodes that are scaled to a proper magnitude. The critical mode is easily obtained for simple cases. For many cases it may very well happen that some relevant eigenmode will have a very high modal number and is therefore hard to find. As the source of imperfection is the welding process it may be simpler to use pre-knowledge of what are possible deformations. The magnitude of initial deformations is often taken as the tolerance given in EN 1090-2. Assuming that the statistical distribution of the initial deformations was known it would be possible to calculate a design value to be used. Systematic measurements are however rarely published, so there is a lack of reliable data [10]. A reduction with a factor of 0.8 is recommended by the code. The influence of residual stress is mostly considered by introducing fictitious initial deformations. However, the direct definition of residual stress can be easily realized with modern software codes. According to EC3, the assumed distribution should correspond to the average course and amplitude that can be expected from the production process. This allows broad latitude for interpretation as the residual stress profile resulting from welding is influenced by a large number of variables.

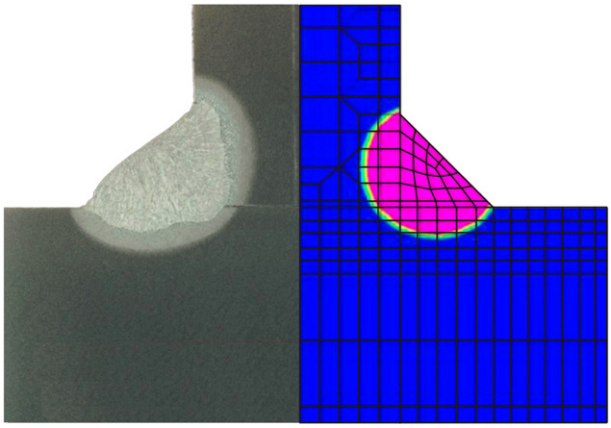

Fig. 8. Comparison of macrosection and simulated weld pool dimensions [1].

4.1. Residual stress models

In the design of steel structures, simplified models are used. Two common engineering models are shown in Fig. 14. The actual stress field is replaced by a trapezoidal or block-like distribution whose borders are determined based on geometrical parameters. For the tension area the maximum stress is expected to reach the yield strength of the base material. The magnitude of the compressive area is calculated based on equilibrium conditions and is assumed to have a constant course. Yet, relevant parameters in terms of the fabrication process or the material itself are neglected. In Fig. 15 the approximated course made in Section 3 is superposed with the models proposed in [11,12]. As it can be seen, none of the investigated models matches the actual stress field.

When comparing both models, the second approach made in [12] led to a more favourable distribution and is therefore recommended. In contrast to the model presented in [11], the amplitude of compressive stress is introduced variable. However, a general review cannot be given, as the comparison is restricted to the examined cases with the parameters given in Table 1. This leads to a more general problem of the simplified models as no information to limit the validity range is given. In order to receive a reliable assessment further investigations are needed, which is the scope of an ongoing project in cooperation with the BAM Federal Institute for Materials Testing and Research, Berlin [2].

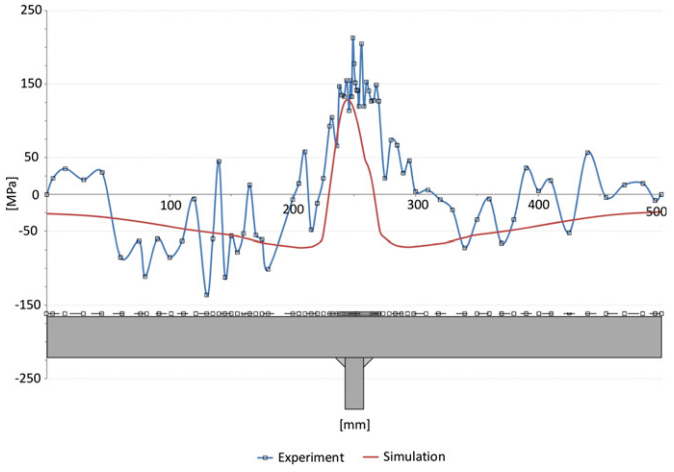

Fig. 9. Comparison of the simulated stress course with residual stress measurements (XRD) for the upper flange.

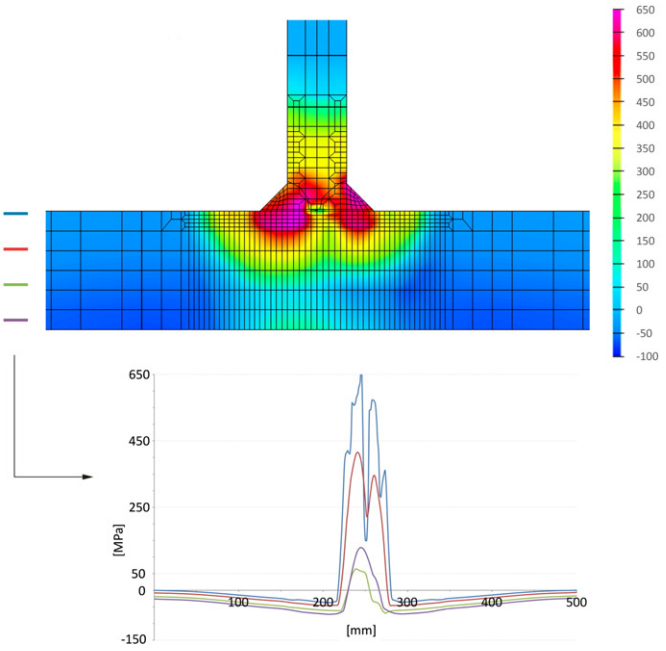

Fig. 10. Calculated longitudinal residual stress state and evaluation for 4 sections over the flange thickness.

The stresses in welded components can be generally divided into restraint stresses resulting from a local shrinkage restraint and reaction stresses as a result of supporting effects. In this article only the former are referred as residual stress as no external fixings or clamping are involved during the manufacture. The source of residual stress (and also distortion) is an inhomogeneous change in volume due to the thermal expansion and shrinkage or as a result of phase transformations (austenite to ferrite–perlite, bainite or martensite) during cooling. Therefore the result depends on the heat input, the restraining conditions in terms of the thickness and also the material as well as the phase transformations. The influence of the latter becomes more visible as the transformation temperature is decreasing. This effect can be noted especially for high strength steel, which is being used more frequently nowadays. Due to the neglect of relevant parameters the extent and magnitude of the residual tension field (and accordingly also the compressive stress) is either approximated wrong or insufficient.

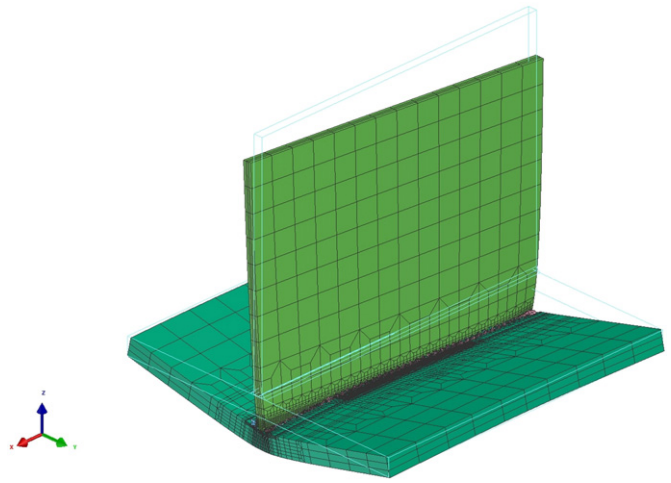

Fig. 12. Total distortion after welding with 50× magnification.

4.2. Distortion

The distortions caused by welding are a result of the longitudinal and transverse shrinkage of the weld area and the HAZ. For a better understanding, the strains are replaced by an imaginary force, generally referred as shrinkage force. Dependent on the point of force application, at the same time bending and angular distortion result to a certain extent. For thin sheets without sufficient bracing there is a risk of additional buckling. The size of distortions mainly depends on the geometry, the supporting conditions and the position of the weld, but also on the material and the heat control. For multiple welds attention should be paid to the welding sequence. For steel constructions, the size of distortions is controlled by compliance with the tolerance values stated in EN 1090-2.

As an example, the simulated value of the web curvature is given and compared to values from the standard (Fig. 16). It can be seen that the standard value is overestimating the extent of distortion. The same conclusion applies to all simulated values, see [1]. The transfer to a load model can be achieved by directly entering the coordinates. This approach is comparatively time consuming and requires the same mesh. The implementation may be simplified by scaling the relevant eigenmode (Fig. 17). For this example the local welding distortion has only little effect.

For the cross section to be investigated in Section 5, the carrying capacity is influenced by the precamber in y and z-direction respectively. The deformation in z-direction along the longitudinal axis is plotted in

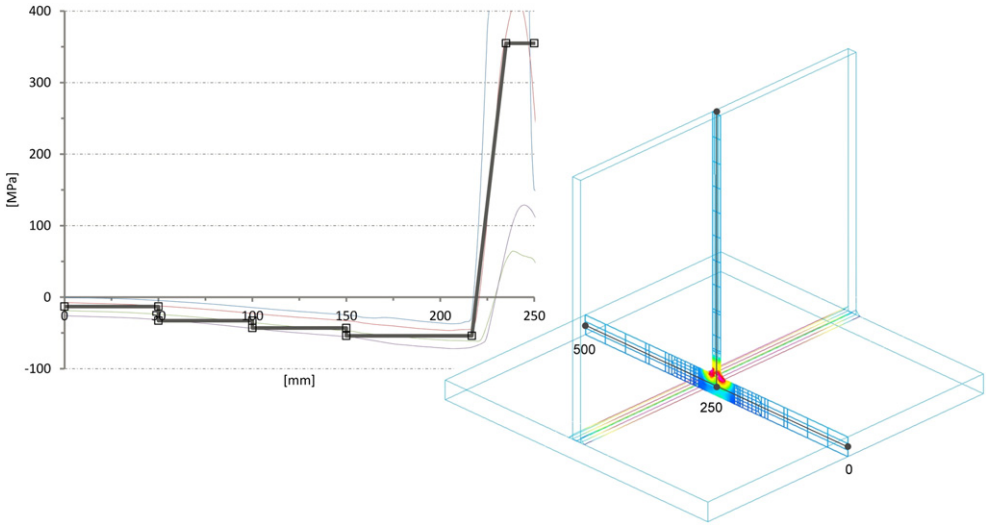

Fig. 11. Approximated residual stress course over the flange width, displayed till x = 250 mm (symmetry).

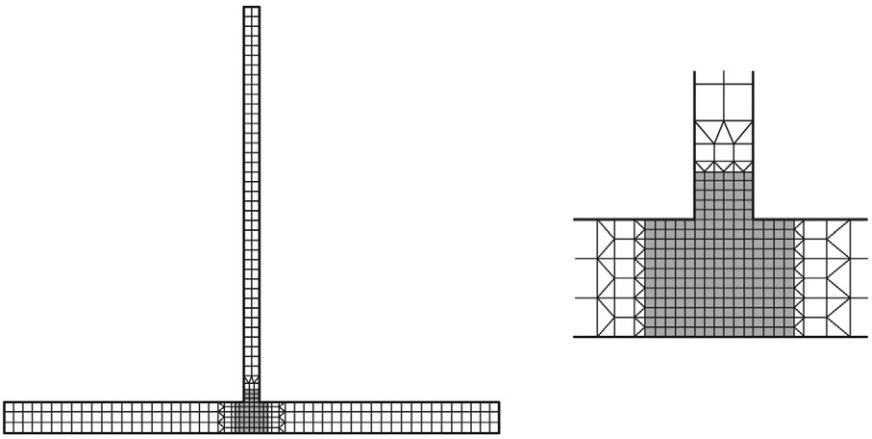

Fig. 13. Numerical model of the half part demonstrator with reduced mesh density 2.5–10 mm, Simufact.

Fig. 18. A line is drawn in between the end points to derive the amplitude (0.12 mm). The tolerance limit corresponds to L/750 multiplied with a factor of 0.8 (0.56 mm). However, it should be noted that the length of the specimens to be investigated in Section 5 is far from the lengths used for the welding simulation model. Hence, this example can only serve as an indicator that the tolerance limit is often overestimating the size of imperfections. In this context the welding sequence is of additional importance. Due to the simplifications in symmetry, the value of bending distortion may experience larger values in a full model with welds deposited one at a time.

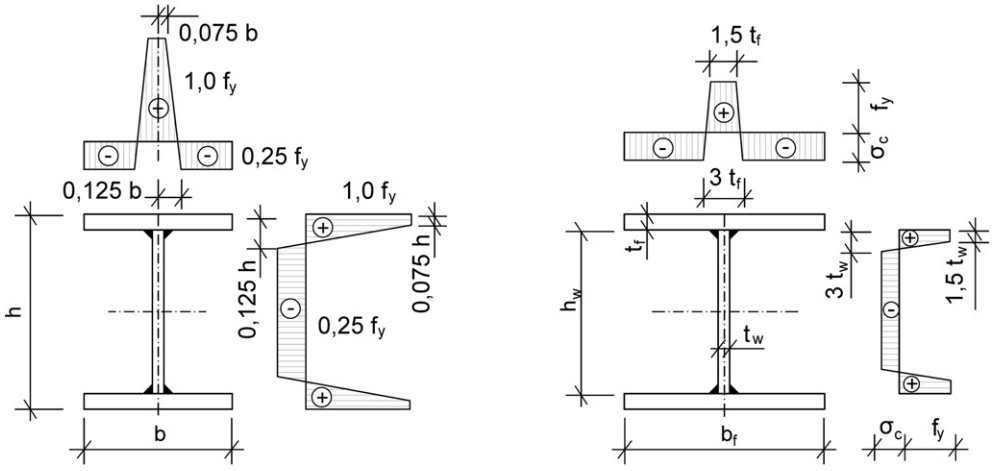

Fig. 14. Simplified residual stress models due to [11] (see a) and [12] (see b).

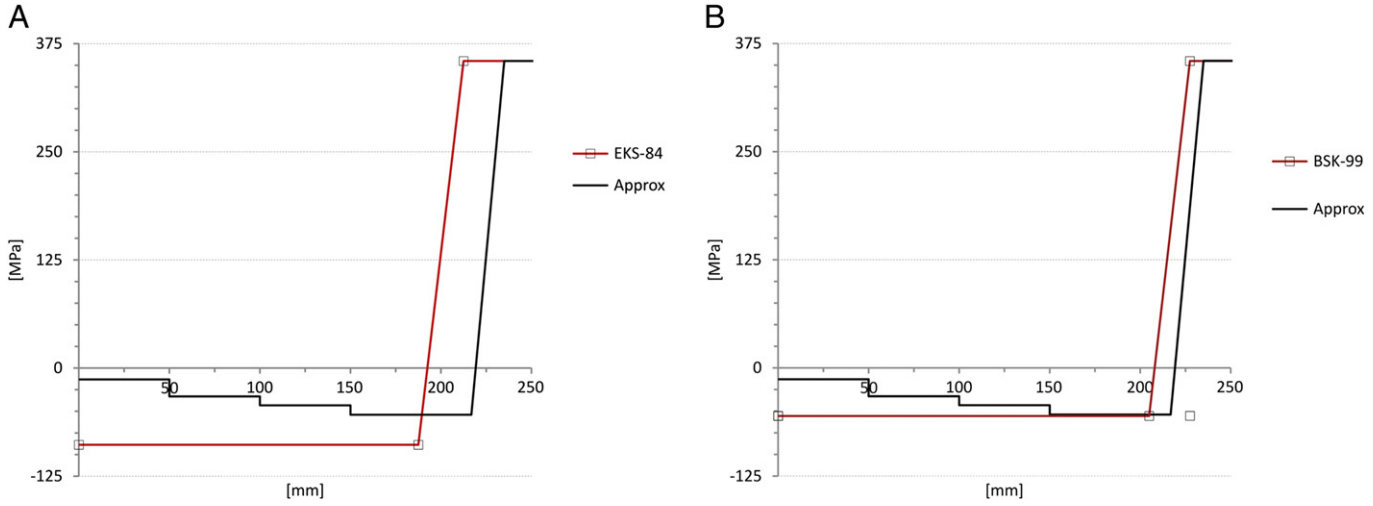

Fig. 15. Comparison between approximated residual stress course (see Fig. 11) and simplified models (see Fig. 14).

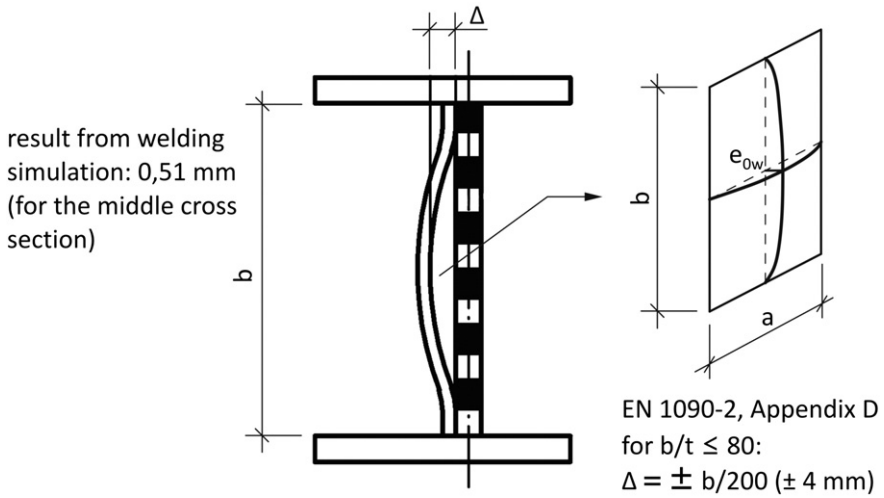

Fig. 16. Tolerance limits for the web curvature according to EN 1090-2.

5. Nonlinear capacity calculations

A geometrically and materially nonlinear calculation allows the most realistic approximation of the load carrying behaviour and thereby more efficient and economical structures. Fig. 19 summarizes the steps for performing such analysis, below referred as GMNIA.

5.1. Input values

The calculation was performed using the software Abaqus, version 6.11–3. Investigations refer to uniform members exposed to axial compression, the length L is varied systematically. Different ratios of relative slenderness are distinguished, indicated as lower (0.6), middle (1.0) and upper (1.4) slenderness range. The following section presents the results for flexural buckling about the minor axis and steel grade S355. The meshing of the geometry was realized using the shell element type S4R, a 4-node element with reduced integration. The average element edge length was chosen with 25 mm. In the following a short overview of input variables is presented:

- Geometry [mm]:
  Cross-section:
  $b_f = 500$, $t_f = 30$, $h_w = 800$, $t_w = 15$
  Length (3 slenderness ratios):
  L1 = 5835, L2 = 9725, L3 = 13,615
- Geometrical Nonlinearity:
  NLGEOM = ON
- Material nonlinearity:
  Elastic–plastic with pseudo hardening
- Geometric Imperfections:
  Precamber: 0.8 × L/750 (global), local distortions (see Fig. 17).
- Combinations:
  1: Gl, 2: Gl + 0.7 L, 3: 0.7Gl + L
- Structural Imperfections:
  RS1: EKS-84 [11], RS2: BSK-99 [12], RS3: Real (see Fig. 11).

The focus of the investigation is the evaluation of the influence of a variation in the residual welding stress. The results are standardized and compared to the relevant buckling curve. Partial safety factors are excluded. Therefore, results can be indicated as characteristic values.

5.2. Evaluation

The benefits connected with a more realistic residual stress approach will be explained based on the comparison of residual stress models RS1 to RS3. In Fig. 20 the results of the relevant combination are plotted. Table 2 shows the corresponding values. It can be seen that the residual stress effect decreases with increasing slenderness. A noticeable effect is restricted to the lower and medium slenderness range. The majority of components in structural engineering practice correspond with that range. In the upper slenderness area geometry effects are dominant.

The values of the FE analysis including the results of welding simulation can be assigned to buckling curve a. A classification to curve c only applies for the approach RS1, which equals a very conservative

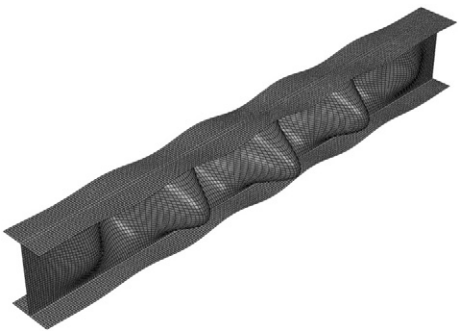

Fig. 17. Approximate implementation of welding distortions by scaling of different eigenmodes.

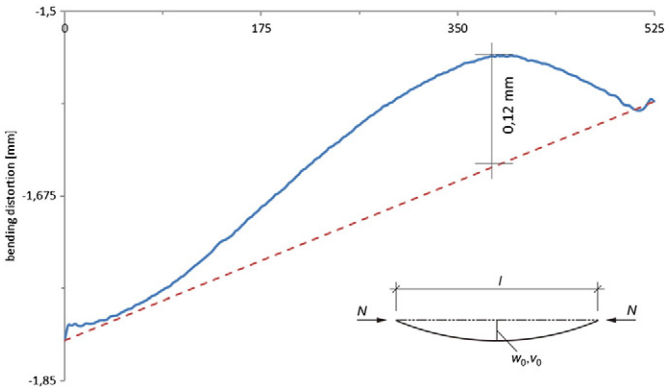

Fig. 18. Simulated bending distortion (in z-direction) along the longitudinal axis [mm], Sysweld.

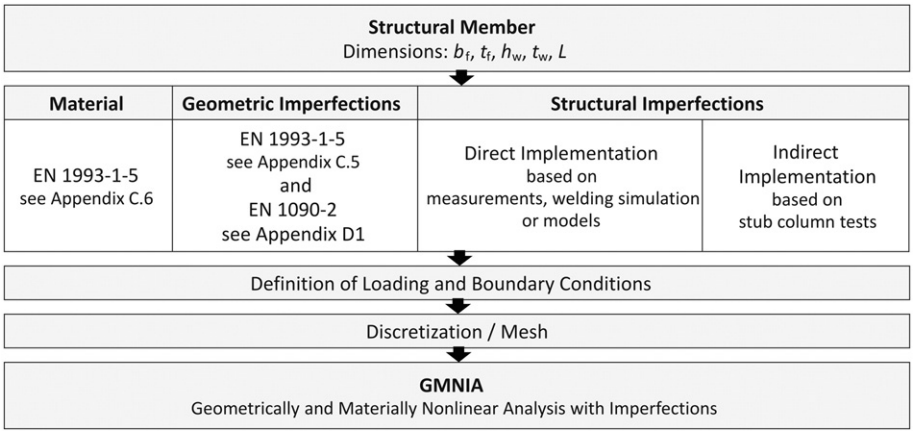

Fig. 19. Geometrically and materially nonlinear imperfection analysis (GMNIA).

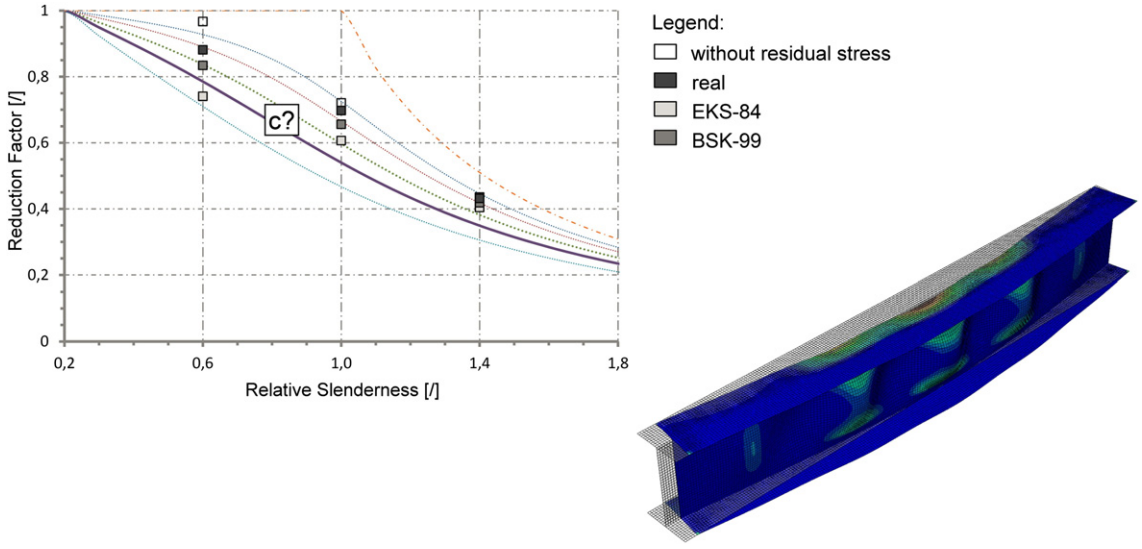

Fig. 20. Results of capacity calculations for flexural buckling about the weak axis, see also Table 2.

approximation of residual stress as previously shown in Section 4. It could be shown that the size of load capacity strongly depends on the residual stress approach. The maximum reduction of capacity was calculated as 24% for RS1, 14% for RS2 and 9% for RS3.

The dominating factors are the magnitude and course of compressive residual stress. Further investigations have proven that deviations generally increase with an increase in yield strength. The application of simplified models is therefore conservative. In order to generalize the results, user-oriented and realistic models need to be provided. This requires a systematic study of different influencing factors. In an ongoing research project these steps are carried out including a wide experimental and numerical program [2].

Table 2
Reduction factor of load capacity for different residual stress models.

	$\lambda = 0,6$	$\lambda = 1,0$	$\lambda = 1,4$
EC3	0785	0540	0349
Without RS	0967	0720	0435
RS1	0741	0606	0404
RS2	0834	0656	0418
RS3	0881	0697	0431

6. Conclusion

The combination of welding simulation and capacity simulation tools holds large potential. However, as the application is still limited to small components, a contemporary introduction to the construction area seems unlikely. For structural engineering, the use of engineering models is adequate. Yet, no sufficient models are available as has been shown by the comparison of welding simulation and simplified models.

For further investigations relevant parameters such as the heat control, the thickness and the material have to be taken into account. For high strength steels it should be noted that existent models may lead to very conservative results as deviations tend to increase for higher material grades [2]. For the revision of standards the results could be included leading to an extended buckling model. The recent classification, being independent of the material and the manufacturing conditions, implies uneconomic design.

Acknowledgment

The authors would like to thank the German Federation of Industrial Research Associations (AiF) for its financial support on the projects IGF-No. 16937 BG and IGF-No. 18104 BG. The projects are carried out

under the auspices of AiF and financed within the budget of the Federal Ministry of Economics and Technology (BMWi) as part of the program to support Industrial Community Research and Development (IGF).

References

[1] K. Dilger, H. Pasternak, et al., Schweißen dicker Bleche unter Baustellenbedingungen – Beurteilung des Einflusses auf das Tragverhalten von Montagestößen (Welding of Thick Plates under Site Conditions – Evaluation of the Influence on the Structure Behaviour of Welded Assembly Joints), Final report, Research project P 858/08/2011/IGF-No. 16937 BG, 2015.
[2] H. Pasternak, T. Kannengießer, et al., Erhöhung der Tragfähigkeit geschweißter I-Profile aus hochfestem Baustahl durch verbesserte Ansätze zur Berücksichtigung von Eigenspannungen (Enhancement of Load Capacity of Welded High-Strength I-Shape Sections Using Improved Design Models for the Consideration of Residual Stress), Ongoing research project P1035/IGF-No. 18104 BG, 2014–2016.
[3] J. Goldak, A. Chakravarti, M. Bibby, A new finite element model for welding heat sources, 15 (2) (1984) 299–305.
[4] J.B. Leblond, J. Devaux, A new kinematic model for anisothermal metallurgical transformations in steels including effect of austenite grain size, Acta Metall. 32 (1) (1984) 137–146.
[5] W.A. Johnson, R.F. Mehl, Reaction kinetics in processes of nucleation and growth, Trans. Metall. Soc. AIME 135 (1939) 416–442.
[6] D. Koistinen, R. Marburger, A general equation prescribing the extent of the austenite–martensite transformation in pure iron-carbon alloys and plain carbon steels, Acta Metall. 7 (1) (1959) 59–60.
[7] U. Peil, M. Wichers, Schweißen unter Betriebsbeanspruchung – Werkstoffkennwerte für einen S355J2G3 unter Temperaturen bis 1200 °C (Trans.: Welding under operating conditions – material characteristics of S355J2G3 at temperatures up to 1200 °C), Stahlbau, 72, 2004 (Nr. 6, S. 400–416).
[8] O. Voß, Untersuchungen relevanter Einflussgrößen auf die numerische Schweißsimulation (Investigation of relevant influencing factors on the numerical welding simulation), (Dissertation) TU Braunschweig, Shaker Verlag, Aachen, 2001.
[9] D. Radaj, Welding Residual Stresses and Distortion: Calculation and Measurement, Woodhead Publishing Limited, 2003.
[10] B. Johansson, R. Maquoi, G. Sedlacek, C. Müller, D. Beg, Commentary and Worked Examples to EN 1993-1–5: Plated Structural Elements, EUR 22898 EN, 2007.
[11] ECCS-CECM-EKS, Publication No. 33: ultimate limit state, calculation of sway frames with rigid joints, 1984 (Brussels).
[12] BSK 99: Swedish Design Rules for Steel Structures, Swedish National Board of Housing, Building and Planning, Boverket, 1999.